On the modeling of modes coupling in dissipative fluid-filled waveguide with corrugated surfaces

Tony Valier-Brasier,[a] Catherine Potel,[b] and Michel Bruneau
Laboratoire d'Acoustique de l'Université du Maine (LAUM), UMR CNRS 6613, Le Mans, France and Fédération Acoustique du Nord-Ouest (FANO), FR CNRS 3110, France

(Received 22 March 2009; accepted 2 July 2009; published online 11 August 2009)

This paper aims at providing an alternative analytical model, which would be more suitable than a previous one [C. Potel and M. Bruneau, J. Sound Vib. **313**, 738 (2008)], to describe the mode coupling due to scattering on small one-dimensional irregularities (parallel ridges) of the surfaces of a fluid-filled waveguide. Both models rely on standard integral formulation and modal analysis, the acoustic field being expressed as a coupling between eigenmodes of a regularly shaped waveguide, which bounds outwardly the corrugated waveguide considered. But the model presented here departs from the previous one essentially because it starts from the integral formulation for the acoustic pressure field, the solution relying on a modal expansion, whereas the previous one starts from the inner product of the set of differential equations (which govern the acoustic pressure field) and the appropriate eigenfunctions, the solution being obtained from using a one-dimensional integral formulation. Substituting this alternative model for the previous one clearly accelerates convergences (even permits to avoid divergences) of the iterative process used to solve the problem. Finally, complex eigenfunctions are introduced here in order to account for the dissipative effects due to thermoviscous phenomena (through an impedancelike boundary condition), which is of importance at the cut-off frequencies. © *2009 American Institute of Physics*.
[DOI: 10.1063/1.3191045]

I. INTRODUCTION

Numerous works on the acoustic propagation inside corrugated waveguide have been carried out for several decades (see Refs. 1–32 and references contained therein). But it is still a challenging topic to obtain tractable and accurate modeling to predict the properties of these fields, having in mind the characterization of the roughness of the boundaries of waveguides. An analytical model proposed recently[23] appears to be more tractable than the previous ones, and suitable to describe the mode coupling due to scattering phenomena on small one-dimensional (1D) irregularities (parallel ridges) of the surfaces of nondissipative fluid-filled waveguides. In this former model,[23] analytic solutions for describing the acoustic coupling in fluid-filled rough waveguides are given, using Green's theorem and perturbation method in the frame of a modal analysis. More precisely, this model relies on standard integral formulation and modal analysis, the acoustic field being expressed as a coupling between a unique set of Neumann eigenmodes of a regularly shaped waveguide, which bounds outwardly the corrugated waveguide considered ("intermodal" approach as opposed to the so-called "multimodal" approach). This model, called here "inner product" (IP) model, starts from the inner product of the set of differential equations (which govern the acoustic pressure field) and the appropriate eigenfunctions, the solution being obtained from using a 1D integral formulation and finally an iterative process to solve the problem. Both the depth and the slope of the profile are taken into account, which leads to identify two coupling mechanisms, respectively, the bulk coupling and the boundary modal coupling.[3]

An alternative analytical model, which would be more suitable than the one mentioned above to describe this modal coupling, is presented in this paper. Fundamentally, it relies on the same analytical formalisms, i.e., integral formulation and intermodal approach based on a unique set of eigenfunctions, both the depth and the slope of the profile being taken into account. But the model presented here, called "integral formulation" (IF) model, departs from the previous one because it starts from the integral formulation for the acoustic pressure field, the solution, which relies on a modal expansion, being finally obtained using also an iterative process. Thus, this alternative approach does not behave like the previous one. More specifically, it appears that it clearly accelerates convergences of the iterative process used to solve the problem; even it permits to avoid divergences. Both models are presented below (Sec. II): the IP model (the previous one) succinctly (Sec. II B) and the IF model (the new one) with more details (Sec. II C). Moreover, complex eigenfunctions are introduced here in each approach in order to account for the dissipative effects due to thermoviscous phenomena (through an impedancelike boundary condition), which is of importance at the cut-off frequencies. Finally, theoretical results are discussed (Sec. III), showing first the role played by the dissipative effects, compared to the effects of the diffusion due to the corrugations, in terms of attenua-

[a]Electronic mail: tony.valier-brasier.etu@univ-lemans.fr.
[b]Author to whom correspondence should be addressed. Tel.: 33 2 43 83 36 17. FAX: 33 2 43 83 35 20. Electronic mail: catherine.potel@univ-lemans.fr.

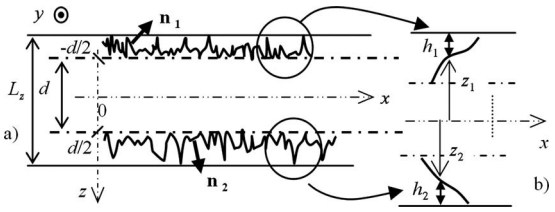

FIG. 1. Sketch of the 2D waveguide with surfaces having small deviations from the regular shape. (a) General view and (b) zoom on the corrugation.

tion of the amplitude of the wave propagating along the waveguide, and second the advantages of the IF model.

II. ANALYTICAL APPROACHES OF THE INTERMODAL COUPLING IN CORRUGATED WAVEGUIDE

A. The waveguide and its boundaries, the fundamental problem

The two-dimensional (2D) (x,z) structure under consideration is shown in Fig. 1. A fluid-filled plate of axis x is bounded by two surfaces having 1D shape perturbations (corrugations parallel to the y-axis) set, respectively, at the coordinates z_1 and z_2 (which depend on the coordinate x). These corrugations are assumed to be small deviations from the regularly shaped surfaces (set at $\pm L_z/2$) bounding outwardly the perturbed surfaces. The distances between both surfaces (the regular one and the corrugated one) are denoted $h_1=(L_z/2)+z_1$ and $h_2=(L_z/2)-z_2$. An inner plate with regularly shaped surfaces $z=\pm d/2$ is defined as being surrounded by the 1D corrugations. The shape of the corrugations is defined by the local unit vectors $\mathbf{n}_1$ and $\mathbf{n}_2$ normal to the real surfaces of the waveguide. The fluid is characterized by its density ρ_0, the adiabatic speed of sound c_0, its shear viscosity coefficient μ_0, and its thermal conduction coefficient λ_0. For air in standard conditions, $\rho_0=1.2$ kg m^{-3}, $\lambda_0/(\rho_0 c_0 C_P)=5.8\times10^{-8}$ m, and $\mu_0/(\rho_0 c_0)=4.7\times10^{-8}$ m where C_P is the heat coefficient at constant pressure per unit of mass of the gas.

In order to account for the reactive and dissipative effects due to thermoviscous phenomena inside the associated boundary layers, the surfaces can also be characterized by an adimensional admittancelike boundary condition $\hat{Y}$, the effects of the viscous factor being replaced here with half of its maximum value (which is very close to its mean value over all the directions of ingoing waves on a plane surface). This admittance, which is of importance at the cut-off frequencies, is given by (for any surface and for any field considered)[33]

$$\hat{Y}=(1+i)\sqrt{k_0/(2\rho_0 c_0)}\left[\sqrt{\mu_0}/2+(\gamma-1)\sqrt{\lambda_0/C_P}\right], \tag{1}$$

where $k_0=\omega/c_0$ is the adiabatic wavenumber (ω being the angular frequency).

It is assumed that an incident harmonic [with a time factor $\exp(i\omega t)$] propagating wave coming from $x\to-\infty$ or a source, which is set at the input of the considered domain (at the entrance $x=0$ of the corrugated waveguide), is such as it creates an acoustic pressure field $\hat{p}(x,z)$ with a given profile in the z-direction. The acoustic pressure field in the waveguide is governed by the set of equations including the propagation equation and the boundary conditions, which takes the following form:

$$(\partial_{xx}^2+\partial_{zz}^2+k_0^2)\hat{p}(x,z)=-\hat{f}(z)\delta(x),\quad \forall x\in(0,\infty),\quad \forall z\in(-L_z/2,L_z/2), \tag{2a}$$

$$(\partial_{n_1}+ik_0\hat{Y})\hat{p}(x,z)=0,\quad \forall x\in(0,\infty),\quad z=z_1, \tag{2b}$$

$$(\partial_{n_2}+ik_0\hat{Y})\hat{p}(x,z)=0,\quad \forall x\in(0,\infty),\quad z=z_2, \tag{2c}$$

$$\text{Sommerfeld condition when } x\to\infty, \tag{2d}$$

where $\hat{f}(z)$ represents the source strength at $x=0$ [$\delta(x)$ being the Dirac function], and where the normal derivatives $\partial_{n_i}(i=1,2)$ are given by

$$\partial_{n_i}=\mathbf{n}_i\cdot\nabla=N_i^{-1}[(\partial_x h_i)\partial_x+(-1)^i\partial_z], \tag{3a}$$

$$\text{with } N_i=\sqrt{(\partial_x h_i)^2+1}. \tag{3b}$$

In both IP and IF approaches presented below, the solution is expressed as an expansion on the eigenfunctions $\hat{\psi}_m^{(\sigma)}(z)$, namely,

$$\hat{p}(x,z)=\sum_{\sigma=1}^{2}\sum_{m=0}^{\infty}\hat{A}_m^{(\sigma)}(x)\hat{\psi}_m^{(\sigma)}(z), \tag{4}$$

where the eigenfunctions $\hat{\psi}_m^{(\sigma)}(z)$ are solutions of the homogeneous Helmholtz equation subject to boundary conditions in the 2D waveguide bounded by the regularly shaped, parallel, and plane surfaces set at $z=\pm L_z/2$ on the outer side of the perturbed surfaces (see the Appendix).

Then, the solutions are given in the frame of a modal theory, using this unique set of eigenmodes of the regularly shaped surface that bounds outwardly the perturbed surface of the waveguide. It is worth noting that the height and the length of the corrugations are here assumed to be such that the perturbation induced by these corrugations on the behavior of the waves propagating along the x-axis is very small.

B. The former IP modeling

Multiplying Eq. (2a) by the eigenfunctions $\hat{\psi}_m^{(\sigma)}(z)$, and integrating over the range $z_1\le z\le z_2$, and then integrating the second term (which includes the operator ∂_{zz}^2) by parts, yield reporting expressions (2b), (2c), (3a), (3b), and (4), respectively, for $\partial_n\hat{p}$ and $\partial_z\hat{p}$ on the boundaries, and $\hat{p}$,[23]

$$\sum_{\alpha=1}^{2}\sum_{\mu=0}^{\infty}\{[\delta_{\mu m}^{(\alpha\sigma)}-\hat{B}_{\mu m}^{(\alpha\sigma)}(x)][\partial_{xx}^2+(\hat{k}_{x_m}^{(\sigma)})^2]+\hat{\gamma}_{\mu m}^{(\alpha\sigma)}(x)\}\hat{A}_\mu^{(\alpha)}(x)=-\hat{S}_m^{(\sigma)}, \tag{5a}$$

where

$$(\hat{k}_{x_m}^{(\sigma)})^2=k_0^2-(\hat{\chi}_m^{(\sigma)})^2,$$

$\hat{\chi}_m^{(\sigma)}$ being the eigenvalue of the mode (σ,m),

$$\delta_{\mu m}^{(\alpha\sigma)} = \delta_{\alpha\sigma}\delta_{\mu m},$$

δ_{rs} being the Kronecker index, (5b)

$$\hat{B}_{\mu m}^{(\alpha\sigma)}(x) = \left(\int_{-L_z/2}^{z_1} \mathrm{d}z + \int_{z_2}^{L_z/2} \mathrm{d}z\right) \hat{\psi}_{\mu}^{(\alpha)}(z)\hat{\psi}_{m}^{(\sigma)}(z) \tag{5c}$$

account for the depth of the roughness (bulk modal coupling),

$$\hat{S}_{m}^{(\sigma)} = \int_{z_1}^{z_2} \hat{\psi}_{m}^{(\sigma)}(z)\hat{f}(z)\mathrm{d}z \tag{5d}$$

represents the energy transfer between the source and the mode (σ,m), and

$$\hat{\gamma}_{\mu m}^{(\alpha\sigma)}(x) = -\sum_{q=1}^{2} \hat{\psi}_{\mu}^{(\alpha)}(z_q)[(\partial_x h_q)\partial_x + ik_0\hat{Y}N_q + (-1)^q\partial_{z_q}]\hat{\psi}_{m}^{(\sigma)}(z_q) \tag{5e}$$

is the operator that represents the boundary modal coupling due to the shape profile of the roughness, its depth, and the thermoviscous boundary layers.

Invoking the following expression for the parameter $\hat{B}_{\mu m}^{(\alpha\sigma)}$, respectively, for $(\alpha,\mu)\neq(\sigma,m)$ and for $(\alpha,\mu)=(\sigma,m)$, straightforwardly obtained from its definition (5c),

$$\hat{B}_{\mu m}^{(\alpha\sigma)}(x) = [(\hat{\chi}_{\mu}^{(\alpha)})^2 - (\hat{\chi}_{m}^{(\sigma)})^2]^{-1}\sum_{q=1}^{2}(-1)^q[\hat{\psi}_{m}^{(\sigma)}(z_q)\partial_{z_q}\hat{\psi}_{\mu}^{(\alpha)}(z_q) - \hat{\psi}_{\mu}^{(\alpha)}(z_q)\partial_{z_q}\hat{\psi}_{m}^{(\sigma)}(z_q)], \tag{6a}$$

$$\hat{B}_{mm}^{(\sigma\sigma)}(x) = 1 - \frac{1}{2}(\hat{N}_{m}^{(\sigma)})^2\sum_{q=1}^{2}(-1)^q[z_q - \hat{N}_{m}^{(\sigma)} \times (2\hat{\chi}_{m}^{(\sigma)})^{-\sigma}\partial_{z_q}^{\sigma-1}\hat{\psi}_{m}^{(\sigma)}(2z_q)]. \tag{6b}$$

Equation (5a) can be written as follows [Eq. (19) of Ref. 23 with different notations]:

$$[\partial_{xx}^2 + (k_{x_m}^{(\sigma)})^2]\hat{A}_{m}^{(\sigma)}(x) = -\hat{S}_{m}^{(\sigma)} + \sum_{\alpha=1}^{2}\sum_{\mu=0}^{\infty}\left\{\sum_{q=1}^{2}\hat{\psi}_{m}^{(\sigma)}(z_q) \times O(x,z_q)\hat{\psi}_{\mu}^{(\alpha)}(z_q) + \hat{B}_{\mu m}^{(\alpha\sigma)}(x)[\partial_{xx}^2 + (k_{x_\mu}^{(\sigma)})^2]\right\}\hat{A}_{\mu}^{(\alpha)}(x), \tag{7a}$$

where the "roughness operator" $O(x,z_q)$ is given by

$$O(x,z_q) = ik_0\hat{Y} + N_q^{-1}[(\partial_x h_q)\partial_x + (-1)^q\partial_{z_q}], \quad q = 1,2. \tag{7b}$$

The approximate integral solution of this equation can be obtained by successive approximations, using at each stage the integral formulation with an appropriate Green's function denoted $g_{m}^{(\sigma)}(x,x')$, namely, here

$$g_{m}^{(\sigma)}(x,x') = \exp(-ik_{x_m}^{(\sigma)}|x-x'|)/(2ik_{x_m}^{(\sigma)}). \tag{8}$$

Using an iterative method to express the amplitude of each mode $\hat{A}_{m}^{(\sigma)}(x)$, which assumes that the coupling function in the right hand side of Eq. (7a) is a small quantity compared to the source term $\hat{S}_{m}^{(\sigma)}$, thus the Nth-order solution of Eq. (7a) for $\hat{A}_{m}^{(\sigma)}(x)$ is written as follows:

$$^{[N]}\hat{A}_{m}^{(\sigma)} = {}^{(0)}\hat{A}_{m}^{(\sigma)} + {}^{(1)}\hat{A}_{m}^{(\sigma)} + \cdots + {}^{(N-1)}\hat{A}_{m}^{(\sigma)} + {}^{(N)}\hat{A}_{m}^{(\sigma)}, \tag{9}$$

where $^{[N]}\hat{A}_{m}^{(\sigma)}$ denotes the Nth-order perturbation expansion for $\hat{A}_{m}^{(\sigma)}$, $^{(0)}\hat{A}_{m}^{(\sigma)}$ the zero order approximation (the solution without roughness), $^{(1)}\hat{A}_{m}^{(\sigma)}$ the first order correction term, and so on.

C. The present IF modeling

The integral formulation of the problem stated above, Eqs. (2a) and (2b), can be written as follows, in the domain $[x\in(0,\infty), z\in(-L_z/2, L_z/2)]$:

$$\left.\begin{array}{ll} x\in(0,\infty), z\in(z_1,z_2), & \hat{p}(x,z) \\ x\in(0,\infty), z\notin(z_1,z_2), & 0 \end{array}\right\} = \int_0^{\infty}\mathrm{d}x'\int_{z_1}^{z_2}\mathrm{d}z' G(x,z;x',z')\hat{f}(z')\delta(x') + \sum_{q=1}^{2}\int_0^{\infty}\mathrm{d}x'[G(x,z;x',z_q)\partial_{n_q}\hat{p}(x',z_q) - \hat{p}(x',z_q)\partial_{n_q}G(x,z;x',z_q)], \tag{10a}$$

where the Green function $G(x,z;x',z')$ is given by the eigenfunction expansion

$$G(x,z;x',z') = \sum_{\alpha=1}^{2}\sum_{\mu=0}^{\infty}[g_{\mu}^{(\alpha)}(x,x')\hat{\psi}_{\mu}^{(\alpha)}(z')]\hat{\psi}_{\mu}^{(\alpha)}(z), \tag{10b}$$

$g_{\mu}^{(\alpha)}(x,x')$ being given by Eq. (8).

Invoking Eqs. (2b), (2c), (3a), (3b), (4), (A1b), and (A1c), Eq. (10a) yields straightforwardly

$$\left.\begin{array}{ll} x\in(0,\infty), z\in(z_1,z_2), & \displaystyle\sum_{\beta=1}^{2}\sum_{\nu=0}^{\infty}\hat{A}_{\nu}^{(\beta)}(x)\hat{\psi}_{\nu}^{(\beta)}(z) \\ x\in(0,\infty), z\notin(z_1,z_2), & 0 \end{array}\right\} = \sum_{\beta=1}^{2}\sum_{\nu=0}^{\infty}\left[\hat{F}_{\nu}^{(\beta)}(x) + \sum_{\alpha=1}^{2}\sum_{\mu=0}^{\infty}\hat{H}_{\mu\nu}^{(\alpha\beta)}[\hat{A}_{\mu}^{(\alpha)}(x)]\right]\hat{\psi}_{\nu}^{(\beta)}(z), \tag{11a}$$

with

$$\hat{F}_{\nu}^{(\beta)}(x) = \int_{z_1}^{z_2}[g_{\nu}^{(\beta)}(x,x')\hat{\psi}_{\nu}^{(\beta)}(z')]\hat{f}(z')\mathrm{d}z', \tag{11b}$$

$$\hat{H}_{\mu\nu}^{(\alpha\beta)}[\hat{A}_{\mu}^{(\alpha)}(x)] = -\sum_{q=1}^{2}\int_{0}^{\infty}\hat{A}_{\mu}^{(\alpha)}(x')\hat{\psi}_{\mu}^{(\alpha)}(z_q)O(x',z_q) \times \hat{\psi}_{\nu}^{(\beta)}(z_q)g_{\nu}^{(\beta)}(x,x')\mathrm{d}x', \quad (11c)$$

$O(x',z_q)$ being the roughness operator (7b).

Then, using the orthogonality properties of the eigenfunctions in the interval $z \in (-L_z/2, L_z/2)$, Eq. (11a) yields

$$\hat{A}_{m}^{(\sigma)}(x) = \hat{F}_{m}^{(\sigma)}(x) + \sum_{\alpha=1}^{2}\sum_{\mu=0}^{\infty}\{\hat{H}_{\mu m}^{(\alpha\sigma)}[\hat{A}_{\mu}^{(\alpha)}(x)] + \hat{B}_{\mu m}^{(\alpha\sigma)}(x)\hat{A}_{\mu}^{(\alpha)}(x)\}, \quad (12)$$

the first term in the right hand side representing the effect of the source on the mode m, the second and third ones representing the effects of the shape and the depth of the roughness [the factor $\hat{B}_{\mu m}^{(\alpha\sigma)}(x)$ is given by Eq. (6)].

Using here also an iterative method to express the amplitude of each mode $\hat{A}_{m}^{(\sigma)}(x)$, which assumes that the coupling function in the right hand side of Eq. (12) is a small quantity compared to the source term $\hat{F}_{m}^{(\sigma)}(x)$, thus the Nth-order solution of Eq. (12) for $\hat{A}_{m}^{(\sigma)}(x)$ is written as given in Eq. (9).

It is worth noting that

$$^{(0)}\hat{A}_{m}^{(\sigma)}(x) = \hat{F}_{m}^{(\sigma)}(x), \quad (13a)$$

$$^{[1]}\hat{A}_{m}^{(\sigma)}(x) = \hat{F}_{m}^{(\sigma)}(x) + \sum_{\alpha=1}^{2}\sum_{\mu=0}^{\infty}[\hat{H}_{\mu m}^{(\alpha\sigma)}(^{(0)}\hat{A}_{\mu}^{(\alpha)}(x)) + \hat{B}_{\mu m}^{(\alpha\sigma)}(x)^{(0)}\hat{A}_{\mu}^{(\alpha)}(x)], \quad (13b)$$

and so on.

III. RESULTS AND DISCUSSIONS

The aim of this section is first of all twofold: (i) to show the role played by the dissipative effects, compared to the effects of the diffusion due to the corrugations, in terms of attenuation of the amplitude of the waves propagating along the waveguide, and (ii) to show that the alternative approach presented in this paper (IF approach) clearly accelerates convergences of the iterative process used to solve the problem (even it permits to avoid divergences) in comparison with the previous approach (IP approach). Then, two examples of results showing the effects of the shape and the depth of the roughness, in the vicinity or not of phonon relationships, are presented, taking advantage of the integral formulation presented in this paper.

A. Effects of dissipative processes at the walls of the waveguide

Accounting for the viscous and thermal boundary layers' attenuation, here through an equivalent admittance $\hat{Y}$ [Eq. (1)], results in a quite weak excess of decreasing of the propagating modes, especially those created by the source of energy, compared to the decreasing due to the energy transfer from these modes to other modes through the diffusion process at the rough wall. The ability of the models presented here to evaluate these dissipative effects on the boundaries is shown in this section for a roughness assumed to be sinusoidal on one boundary (using Fourier analysis would then permit to consider any geometry). The values of the adimensional parameters used are given in Table I, where f is the frequency, d is the thickness of the regularly shaped surfaces' inner fluid plate, c_0 is the adiabatic speed of sound, Λ is the spatial wavelength of the sinusoidal roughness, k_0 is the adiabatic wavenumber, ℓ is the total length of the roughness, λ is the acoustic wavelength, and h is the depth of the roughness. The incident wave is assumed to behave as the antisymmetrical mode $m=0$. Three other modes, created by couplings due to the roughness, are accounted for in the calculus: the evanescent antisymmetrical mode $\mu=1$, and two propagative modes, respectively, the symmetrical one $\mu=0$ and the symmetrical one $\mu=1$. The driving frequency is such as the following phonon relationship is approximately verified:

$$k_{x_{\mu=0}}^{(2)} + k_{x_{m=0}}^{(1)} - 2\pi/\Lambda = 0, \quad (14)$$

as shown in Fig. 2 (vertical straight line at $fd/c_0=1.3$).

TABLE I. Parameters used to calculate the results presented in Figs. 2, 3(a), and 3(d) (the notations are given in the text).

$fd/c_0=1.3$	$\Lambda/\lambda=0.52$	$k_0\ell=245$
$d/\Lambda=2.5$	$h/d=0.01$	$\ell/\Lambda=75$

The amplitudes of the modes considered here are shown in Figs. 3(a) and 3(b) as functions of the adimensional distance from the entrance of the rough part of the waveguide k_0x. Because the curves with thermoviscous boundary layers and those without dissipation effects are very close one to the other (as mentioned above), a third curve (the lower one) is presented, which corresponds to an admittance of the walls 20 times higher than the real one $\hat{Y}$ for air under standard conditions.

The amplitude of the incident antisymmetrical mode $m=0$ [Fig. 3(a)] decreases more or less (depending on the dissipative effects) when this mode propagates. The symmetrical mode $\mu=0$ [Fig. 3(b)] is created from the incoming wave

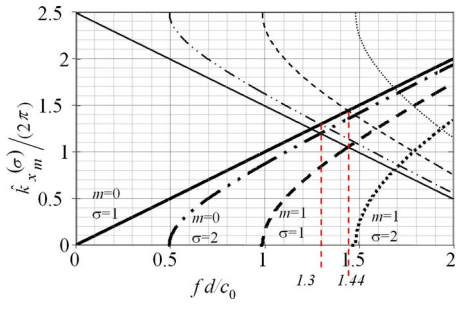

FIG. 2. (Color online) Dispersion curves (thick lines) of the guide with smooth interfaces $\{\hat{k}_{x_m}^{(\sigma)}d/(2\pi)=\sqrt{(fd/c_0)^2-[(2m+\delta_{\sigma 1})d/(2L_z)]^2}\}$, and curves (thin lines) corresponding to the phonon relation (14) $\{\hat{k}_{x_m}^{(\sigma)}d/(2\pi) = d/\Lambda-\sqrt{(fd/c_0)^2-[(2m+\delta_{\sigma 1})d/(2L_z)]^2}\}$, $\sigma=1$ and $\sigma=2$ corresponding, respectively, to antisymmetric and symmetric modes. Solid lines: mode $(m,\sigma)=(0,1)$, dashed-dotted lines: mode $(m,\sigma)=(0,2)$, dashed lines: $(m,\sigma)=(1,1)$, and dotted lines: $(m,\sigma)=(1,2)$.

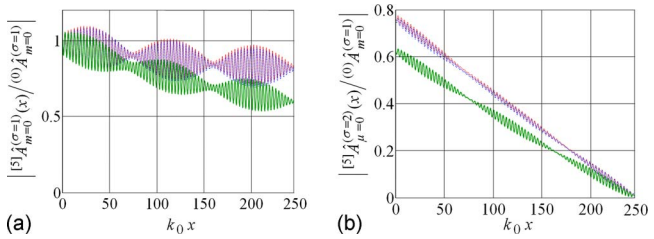

FIG. 3. (Color online) Relative amplitudes of the modes (rear the amplitude of the incoming mode) as functions of the adimensional distance from the entrance of the rough part of the waveguide k_0x, without dissipation (thin solid line), with dissipative thermoviscous boundary layers (for air under standard conditions, dotted line), and with an admittance of the walls 20 times higher time than the real one (thick solid line). (a) Incident antisymmetrical mode $m=0$, and (b) symmetrical mode $\mu=0$ satisfying the phonon relationship (14).

(initial mode generated by the source) by the diffusion process along the corrugation; its amplitude increases when propagating backward, i.e., from the right to the left (counterpropagating wave) and actually its attenuation due to the dissipative process increases also from the right to the left. Its relative amplitude (rear to the amplitude of the incident mode) is quite high because it is linked with the incoming mode by the phonon relationship (14). The amplitudes of the two other modes considered, the antisymmetrical mode $\mu=1$ and the symmetrical mode $\mu=1$, are much lower than the incident mode (less than 4% of the amplitude of the incident mode) because the first one is evanescent and the second one is not linked with any other mode by a phonon relationship.

B. Convergence of the iterative processes

In this section, the convergence of the iterative processes used to solve the problem is analyzed in both cases: the first one when using the previous approach (IP approach), and the second one when using the approach presented in this paper (the IF approach). In the example given here, the roughness is assumed to be a periodically corrugated surface (regularly distributed symmetrical sawtooth profile) on one boundary (Fig. 4). The values of the adimensional parameters used are given in Table II, the notations being the same as those used in Table I.

The incident wave is assumed to behave as the symmetrical mode $m=1$. Three other modes, created by couplings due to the roughness, are accounted for in the calculus: the antisymmetrical modes $\mu=0$ (propagative) and $\mu=1$ (evanescent), and the symmetrical mode $\mu=0$ (propagative). The driving frequency is such as the following phonon relationship between the symmetrical modes $m=1$ and $\mu=0$ is approximately verified:

$$k_{x_{m=1}}^{(2)} + k_{x_{\mu=0}}^{(2)} - 2\pi/\Lambda = 0, \tag{15}$$

as shown in Fig. 2 (vertical straight line at $fd/c_0=1.44$).

The amplitudes of the modes considered here are shown in Figs. 5(a)–5(d) as functions of the adimensional distance from the entrance of the rough part of the waveguide k_0x. The amplitude of the symmetrical mode $\mu=0$, linked with the incident mode (symmetrical mode $m=1$) by the phonon relationship (15), is obtained after 2 or 3 iterations with the IF method [Fig. 5(a)] whereas it is obtained after about 30 iterations with the IP method [Fig. 5(b)]. In the same manner, the amplitude of the incident mode (symmetrical mode $m=1$) is obtained after 2 or 3 iterations with the IF method [Fig. 5(c)] whereas it is obtained after about 30 iterations with the IP method [Fig. 5(d)]. Note that at the lower order, the result obtained for this incident mode using the IP method is divergent (it is not the case when using the IF approach). The amplitudes of the two other modes considered, the antisymmetrical modes $\mu=1$ (evanescent) and $\mu=0$ (propagative), are much lower than the incident mode (less than 4% of the amplitude of the incident mode) because the first one is evanescent and the second one is not linked with any other mode by a phonon relationship.

TABLE II. Parameters used to calculate the results presented in Figs. 5(a)–5(d).

$fd/c_0=1.44$	$\Lambda/\lambda=0.58$	$k_0\ell=181.46$
$d/\Lambda=2.5$	$h/d=0.02$	$\ell/\Lambda=50$

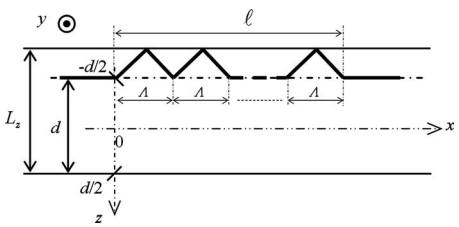

FIG. 4. Fluid plate between two rigid walls: a wall being plane and a wall having regularly distributed corrugation (symmetrical sawtooth profile).

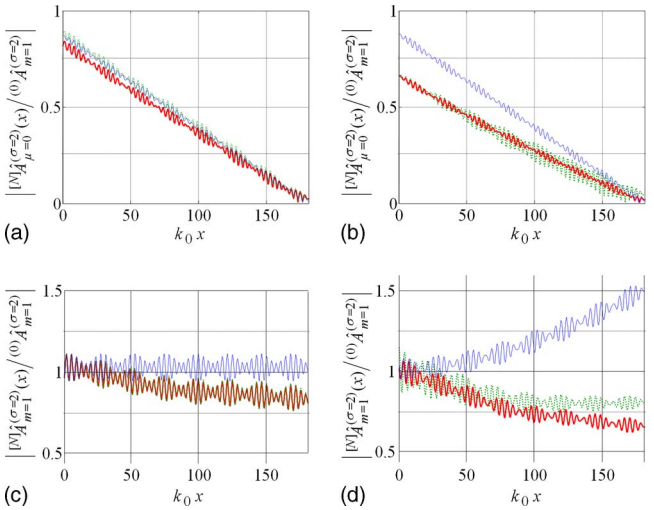

FIG. 5. (Color online) Relative amplitudes of the symmetrical modes $\mu=0$ and $m=1$ (rear the amplitude of the incoming mode) as functions of the adimensional distance from the entrance of the rough part of the waveguide k_0x: normalized modulus of the amplitude of the symmetrical mode $\mu=0$ ${}^{[N]}\hat{A}_{\mu=0}^{(2)}$ calculated to the Nth order, (a) using the IF method with $N=1$ (thin solid line), 2 (dotted line), and 3 (thick solid line), and (b) using the IP method with $N=1$ (thin solid line), 15 (dotted line), and 30 (thick solid line); normalized modulus of the amplitude of the symmetrical mode $m=1$ ${}^{[N]}\hat{A}_{m=1}^{(2)}$ calculated to the Nth order, (c) using the IF method with $N=1$ (thin solid line), 2 (dotted line), and 3 (thick solid line), and (d) using the IP method with $N=1$ (thin solid line), 15 (dotted line), and 30 (thick solid line).

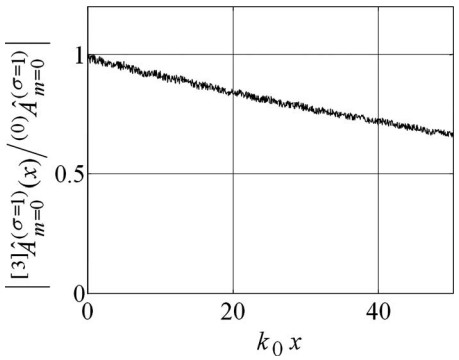

FIG. 6. Relative amplitudes of the incident antisymmetrical mode $m=0$ as functions of the adimensional distance from the entrance of the rough part of the waveguide $k_0 x$.

These results show that the alternative approach presented in this paper (IF approach) clearly accelerates convergences of the iterative process (even it permits to avoid divergences) in comparison with the previous approach (IP approach).

C. Examples of effects of roughnesses

Two examples of results showing the effects of the shape and the depth of the roughness, in the vicinity or not of phonon relationships, are presented in this section, taking advantage of the IF presented in this paper.

In the first one, the roughness is assumed to be randomly distributed on one boundary. The values of the adimensional parameters are such that $fd/c_0=0.8$, $k_0\ell=50$, and $h/d=0.02$. The incident wave is assumed to behave as the antisymmetrical mode $m=0$. Three other modes, created by couplings due to the roughness, are accounted for in the calculus: the evanescent antisymmetrical mode $\mu=1$, and two symmetrical propagative modes, respectively, $\mu=0$ and $\mu=1$. The relative amplitudes of the incident antisymmetrical mode $m=0$ as functions of the adimensional distance from the entrance of the rough part of the waveguide $k_0 x$ are shown in Fig. 6. The amplitudes of the other modes are always much lower than the amplitude of the incoming mode (less than 0.04 time lower) because no phonon relationship occurs here. As expected, the amplitude of the incident mode decreases regularly when propagating along the randomly shaped roughness.

In the second example, the roughness is assumed to be sinusoidal on one boundary. The values of the adimensional parameters are given in Table III. The incident wave is assumed to behave as the antisymmetrical mode $m=0$. Three other modes, created by couplings due to the roughness, are accounted for in the calculus: the antisymmetrical mode $\mu=1$, and two symmetrical propagative modes, respectively, $\mu=0$ and $\mu=1$. As examples, Figs. 7(a) and 7(b) show the relative amplitudes of the incident antisymmetrical mode $m=0$ and of the antisymmetrical mode $\mu=1$ as functions of two coordinates, the adimensional frequency in the range $fd/c_0 \in (1.2, 1.8)$ and the adimensional distance from the entrance of the rough part of the waveguide $X=x/\Lambda \in (0, 10)$, satisfying, respectively, the phonon relationships

$$k_{x_{m=0}}^{(1)} + k_{x_{m=0}}^{(1)} - 2\pi/\Lambda = 0 \tag{16}$$

and

$$k_{x_{m=0}}^{(1)} + k_{x_{\mu=1}}^{(1)} - 2\pi/\Lambda = 0 \tag{17}$$

(the color scale is given in the figures).

TABLE III. Parameters used to calculate the results presented in Figs. 7(a) and 7(b).

$fd/c_0 \in (1.2, 1.8)$	$d/\Lambda=2.5$	$h/d=0.02$	$\ell/\Lambda=10$

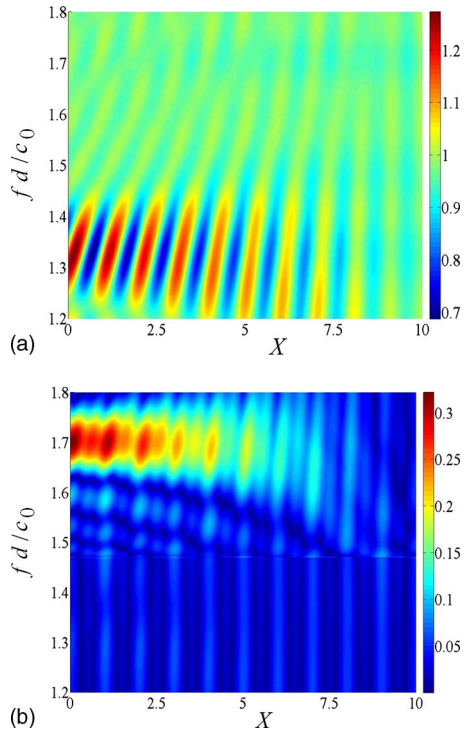

FIG. 7. (Color online) Relative amplitudes of modes as functions of two coordinates: the adimensional frequency in the range $fd/c_0 \in (1.2, 1.8)$ and the adimensional distance from the entrance of the rough part of the waveguide $X=x/\Lambda \in (0, 10)$. (a) Relative amplitude of the incident antisymmetrical mode $m=0$ satisfying the phonon relationship (16), and (b) relative amplitude of the antisymmetrical mode $\mu=1$ satisfying the phonon relationship (17).

The amplitudes of the other modes are always much lower than the amplitude of the incoming mode because they do not obey to phonon relationship in the frequency range considered here.

The spatial period Λ (adimensional length equal to 1 on the horizontal scale) appears clearly in both Figs. 7(a) and 7(b), even for evanescent modes [lower part of Fig. 7(b)]. The upper part of Fig. 7(b) shows a relative value of the amplitude, which is quite high (nearly the third of the value of the amplitude of the incident mode) because at these frequencies the phonon relationship (17) occurs for this mode.

IV. CONCLUSIONS

The results described in this paper indicate that the new approach suggested (IF approach) can lead to substantial improvements, compared to a previous approach (IP approach), in the convergence of the iterative process used to calculate the effect of the roughness of the wall on the wave propaga-

tion in a fluid-filled waveguide. For example, when only $N=1$ iteration is sufficient when using the IF approach, about 30 are needed when using the previous IP approach. Moreover, dissipative effects at the walls have been introduced in both formalisms, which permit to account for the attenuation due to nonvanishing admittance of the wall. Finally, the results show that important aspects, for both propagative and evanescent waves, satisfying or not phonon relationship, can be investigated in detail.

ACKNOWLEDGMENTS

Support from the CNRS through the research group GDR-2501 is gratefully acknowledged. The authors also want to thank their colleagues in the "Fédération d'Acoustique du Nord Ouest" (FANO) for their helpful discussions.

APPENDIX: 1D EIGENMODES OF THE FLUID PLATE SATISFYING MIXED BOUNDARY CONDITIONS

The 1D orthogonal, normalized, respectively, antisymmetrical ($\sigma=1$) and symmetrical ($\sigma=2$) eigenfunctions $\hat{\psi}_m^{(\sigma)}$ considered (with associated eigenvalues $\hat{\chi}_m^{(\sigma)}$) of the 2D waveguide bounded by the regularly shaped, parallel, and plane surfaces set at $z=-L_z/2$ and $z=L_z/2$ are solutions of the homogeneous wave equation and subjected to mixed boundary conditions given by

$$[\partial_{zz}^2+(\hat{\chi}_m^{(\sigma)})^2]\hat{\psi}_m^{(\sigma)}(z)=0, \quad z\in(-L_z/2,L_z/2), \tag{A1a}$$

$$(\partial_z-ik_0\hat{Y})\hat{\psi}_m^{(\sigma)}(z)=0, \quad z=-L_z/2, \tag{A1b}$$

$$(\partial_z+ik_0\hat{Y})\hat{\psi}_m^{(\sigma)}(z)=0, \quad z=L_z/2, \tag{A1c}$$

where it is assumed that the adimensional admittance $\hat{Y}$, which accounts for the effects of thermoviscous boundary layers, does not depend on the quantum number m (the viscous term is replaced with its mean value over all incident angles).[33]

The orthogonality of these eigenfunctions can be verified by integrating from $z=-L_z/2$ to $z=L_z/2$ the following equation:

$$\partial_z(\hat{\psi}_m^{(\sigma)}\partial_z\hat{\psi}_n^{(\sigma)}-\hat{\psi}_n^{(\sigma)}\partial_z\hat{\psi}_m^{(\sigma)})=[(\hat{\chi}_m^{(\sigma)})^2-(\hat{\chi}_n^{(\sigma)})^2]\hat{\psi}_m^{(\sigma)}\hat{\psi}_n^{(\sigma)} \tag{A2}$$

and by noting that the left hand side vanishes because the eigenfunctions satisfy the boundary conditions (A1b) and (A1c).

The normalization of the eigenfunctions is then obtained from the following integral:

$$\int_{-L_z/2}^{L_z/2}\hat{\psi}_m^{(\sigma)}(z)\hat{\psi}_\mu^{(\alpha)}(z)\mathrm{d}z=\delta_{\mu m}^{(\alpha\sigma)}, \tag{A3}$$

$\delta_{\mu m}^{(\alpha\sigma)}=\delta_{\alpha\sigma}\delta_{\mu m}$, δ_{rs} being the Kronecker index, which leads to the following expressions for the solutions of Eqs. (A1a)–(A1c), namely,

$$\hat{\psi}_m^{(1)}(z)=(\hat{N}_m^{(1)})^{-1}\sin(\hat{\chi}_m^{(1)}z), \tag{A4a}$$

$$\hat{\psi}_m^{(2)}(z)=(\hat{N}_m^{(2)})^{-1}\cos(\hat{\chi}_m^{(2)}z), \tag{A4b}$$

with

$$\hat{N}_m^{(\sigma)}=\sqrt{\frac{L_z}{2}+\frac{1}{\hat{\chi}_m^{(\sigma)}}\frac{ik_0\hat{Y}/\hat{\chi}_m^{(\sigma)}}{1-(k_0\hat{Y}/\hat{\chi}_m^{(\sigma)})^2}}, \tag{A4c}$$

the eigenvalues $\hat{\chi}_m^{(\sigma)}$, $(\sigma=1,2)$ being solutions of the following equations:

$$-\frac{\hat{\chi}_m^{(1)}}{ik_0\hat{Y}}=\tan(\hat{\chi}_m^{(1)}L_z/2), \tag{A4d}$$

$$\frac{ik_0\hat{Y}}{\hat{\chi}_m^{(2)}}=\tan(\hat{\chi}_m^{(2)}L_z/2). \tag{A4e}$$

When the admittance $\hat{Y}$ vanishes, relations (A4a)–(A4e) give the well-known Neumann eigenfunctions and eigenvalues

$$\hat{\psi}_m^{(1)}(z)=\sqrt{2/L_z}\sin(k_m^{(1)}z), \tag{A5a}$$

$$\hat{\psi}_m^{(2)}(z)=\sqrt{(2-\delta_{m0})/L_z}\cos(k_m^{(2)}z), \tag{A5b}$$

with

$$k_m^{(1)}=(2m+1)\pi/L_z, \tag{A5c}$$

$$k_m^{(2)}=2m\pi/L_z. \tag{A5d}$$

Because in practice the modulus of the adimensional admittance $\hat{Y}$ is very small, i.e.,

$$|ik_0\hat{Y}|\ll|\hat{\chi}_m^{(\sigma)}|\text{or}|ik_0\hat{Y}|\ll k_m^{(\sigma)}, \quad (\sigma,m)\neq(2,0), \tag{A6}$$

Eqs. (A4d) and (A4e) lead to the following expressions for the eigenvalues:

$$\hat{\chi}_m^{(\sigma)}=k_m^{(\sigma)}+\hat{\varepsilon}_m^{(\sigma)} \tag{A7a}$$

with

$$\hat{\varepsilon}_m^{(\sigma)}=\sqrt{2ik_0\hat{Y}/L_z}, \quad (\sigma,m)=(2,0), \tag{A7b}$$

$$\hat{\varepsilon}_m^{(\sigma)}=2ik_0\hat{Y}/(k_m^{(\sigma)}L_z), \quad (\sigma,m)\neq(2,0), \tag{A7c}$$

and the normalization factors can be approximated by those which appear in Eqs. (A5a) and (A5b).

[1] J. Missaoui and L. Cheng, J. Acoust. Soc. Am. **101**, 3313 (1997).
[2] Y. Y. Li and L. Cheng, J. Acoust. Soc. Am. **116**, 3312 (2004).
[3] K. S. Sum and J. Pan, J. Acoust. Soc. Am. **119**, 2201 (2006).
[4] S. Banerjee and T. Kundu, J. Acoust. Soc. Am. **119**, 2006 (2006).
[5] D. H. Berman, J. Acoust. Soc. Am. **105**, 672 (1999).
[6] O. I. Lobkis and D. E. Chimenti, J. Acoust. Soc. Am. **102**, 143 (1997).
[7] D. E. Chimenti and O. I. Lobkis, Ultrasonics **36**, 155 (1998).
[8] B. I. Boyanov and V. L. Strashilov, IEEE Trans. Ultrason. Ferroelectr. Freq. Control **39**, 119 (1992).
[9] M. A. Hawwa, J. Acoust. Soc. Am. **102**, 137 (1997).
[10] D. H. Berman, J. Acoust. Soc. Am. **96**, 417 (1994).
[11] D. Leduc, A.-C. Hladky, B. Morvan, J.-L. Izbicki, and P. Pareige, J. Acoust. Soc. Am. **118**, 2234 (2005).
[12] A. Boström, J. Acoust. Soc. Am. **85**, 1549 (1989).
[13] A. El-Bahrawy, J. Sound Vib. **170**, 145 (1994).
[14] N. F. Declercq, J. Degrieck, R. Briers, and O. Leroy, Ultrasonics **43**, 605 (2005).
[15] T. Kundu, S. Banerjee, and K. V. Jata, J. Acoust. Soc. Am. **120**, 1217

(2006).
[16]S. Banerjee and T. Kundu, Int. J. Solids Struct. **43**, 6551 (2006).
[17]Y. Y. Lu, J. Huang, and J. McLaughlin, Wave Motion **34**, 193 (2001).
[18]B. Nilsson, Proc. R. Soc. London, Ser. A **458**, 1555 (2002).
[19]A. Jungman, L. Adler, J. D. Achenbach, and R. Roberts, J. Acoust. Soc. Am. **74**, 1025 (1983).
[20]K. Mampaert and O. Leroy, J. Acoust. Soc. Am. **83**, 1390 (1988).
[21]W. Lauriks, L. Kelders, and J. F. Allard, Ultrasonics **36**, 865 (1998).
[22]A. A. Maradudin and D. L. Mills, Ann. Phys. **100**, 262 (1976).
[23]C. Potel and M. Bruneau, J. Sound Vib. **313**, 738 (2008).
[24]C. Potel, D. Leduc, B. Morvan, C. Depollier, A.-C. Hladky-Hennion, J. L. Izbicki, P. Pareige, and M. Bruneau, J. Appl. Phys. **104**, 074908 (2008).
[25]C. Potel, D. Leduc, B. Morvan, C. Depollier, A.-C. Hladky-Hennion, J. L. Izbicki, P. Pareige, and M. Bruneau, J. Appl. Phys. **104**, 074909 (2008).
[26]T. Valier-Brasier, C. Potel, and M. Bruneau, Appl. Phys. Lett. **93**, 164101 (2008).
[27]B. Morvan, A.-C. Hladky-Hennion, D. Leduc, and J. L. Izbicki, J. Appl. Phys. **101**, 114906 (2007).
[28]R. F. Salant, J. Acoust. Soc. Am. **53**, 504 (1973).
[29]J. Clifton Samuels, J. Acoust. Soc. Am. **31**, 319 (1959).
[30]A. H. Nayfeh, J. Acoust. Soc. Am. **56**, 768 (1974).
[31]J. A. Sánchez-Gil, V. D. Freilikher, A. A. Maradudin, and I. Yurkevich, Phys. Rev. B **59**, 5915 (1999).
[32]M. Spivack, J. Acoust. Soc. Am. **101**, 1250 (1997).
[33]M. Bruneau and T. Scelo, *Fundamentals of Acoustics* (ISTE, London, 2006).